MOLECULAR AND CELLULAR BIOLOGY, Dec. 2005, p. 10352–10364 Vol. 25, No. 23
0270-7306/05/$08.00+0 doi:10.1128/MCB.25.23.10352–10364.2005

The Putative NTPase Fap7 Mediates Cytoplasmic 20S Pre-rRNA Processing through a Direct Interaction with Rps14†

Sander Granneman,[1] Madhusudan R. Nandineni,[1] and Susan J. Baserga[1,2,3]*

Departments of Molecular Biophysics and Biochemistry,[1] Genetics,[2] and Therapeutic Radiology,[3] Yale University School of Medicine, New Haven, Connecticut 06520

Received 19 April 2005/Returned for modification 25 May 2005/Accepted 13 September 2005

One of the proteins identified as being involved in ribosome biogenesis by high-throughput studies, a putative P-loop-type kinase termed Fap7 (YDL166c), was shown to be required for the conversion of 20S pre-rRNA to 18S rRNA. However, the mechanism underlying this function has remained unclear. Here we demonstrate that Fap7 is strictly required for cleavage of the 20S pre-rRNA at site D in the cytoplasm. Genetic depletion of Fap7 causes accumulation of only the 20S pre-rRNA, which could be detected not only in 43S preribosomes but also in 80S-sized complexes. Fap7 is not a structural component of 43S preribosomes but likely transiently interacts with them by directly binding to Rps14, a ribosomal protein that is found near the 3′ end of the 18S rRNA. Consistent with an NTPase activity, conserved residues predicted to be required for nucleoside triphosphate (NTP) hydrolysis are essential for Fap7 function in vivo. We propose that Fap7 mediates cleavage of the 20S pre-rRNA at site D by directly interacting with Rps14 and speculate that it is an enzyme that functions as an NTP-dependent molecular switch in 18S rRNA maturation.

In eukaryotes, rRNA transcription and ribosome biogenesis occur in a subnuclear compartment called the nucleolus. In this subcompartment, RNA polymerase I transcribes an rRNA precursor (pre-rRNA) that harbors the 18S, 25S/28S, and 5.8S rRNAs and several noncoding internal and external transcribed spacers (ITS and ETS, respectively) (Fig. 1). The pre-rRNA is chemically modified and cleaved by endo- and exonucleases to produce the mature rRNAs. This process has been most extensively characterized in the yeast *Saccharomyces cerevisiae* (for detailed reviews, see references 36 and 46). In this organism, the primary 35S pre-rRNA is cleaved at sites A_0, A_1, and A_2 to yield the 20S and $27SA_2$ pre-rRNA intermediates. These cleavage steps are mediated by components of the ~80S small-subunit (SSU) processome/90S preribosomes (4, 18). The 20S pre-rRNA, packaged into 43S preribosomes, is exported to the cytoplasm, where it is dimethylated by Dim1 and processed at site D to form the mature 18S rRNA and thereby the 40S ribosomal subunit (SSU). The $27SA_2$ pre-rRNAs, part of 66S preribosomes, can be processed via two pathways leading to the synthesis of the 5.8S and 25S large-subunit (LSU) rRNAs (Fig. 1). Finally, the 5S rRNA is independently transcribed as a precursor by RNA polymerase III (Fig. 1). Many of the cleavage steps in pre-rRNA processing are believed to be endonucleolytic; thus far, however, the enzymes responsible for most of these cleavages have not been identified. Two well-studied examples are the RNase MRP snoRNP, which cleaves at site A_3, and Rnt1, an endonuclease responsible for cleavage of the 3′ ETS (24, 30). One possible candidate for the cleavage at site D in the 20S pre-rRNA is Nob1, a protein that contains a putative PIN domain, which shares structural homology with several exonucleases and flap endonucleases (2, 6, 8). Consistent with a role as a nuclease, conserved residues within the PIN domain are shown by genetic studies to be essential for its function (8). However, it remains unclear whether Nob1 has endonucleolytic activity.

Large-scale proteomic and genomic studies have identified over 150 pre-rRNA-processing factors and numerous preribosomal complexes (11, 36). Peng et al. devised a genome-wide microarray approach to reveal yeast proteins involved in RNA metabolism (35). They identified a large number of proteins required for ribosome biogenesis, including many that had not yet been studied. One of them, Fap7, is an essential nuclear and cytoplasmic protein previously identified in a genetic screen for factors required for activation of a reporter construct during oxidative stress (21, 23). Fap7 belongs to a novel family of P-loop kinases, designated AD-004/AF2001-type kinases of unknown function (21, 28). This family of kinases is related to ribonucleoside kinases and harbors Walker A, an hhh(DE)XH-type Walker B motif characteristic for NTPases (h represents any hydrophobic residue), and a conserved arginine or lysine that is predicted to play an important role in the binding of the α-phosphates of ribonucleosides. There is also considerable evidence suggesting a role in ribosome biogenesis for Fap7: it has been copurified with tandem affinity purification (TAP)-tagged Enp1 (Enp1-TAP) (14), a protein predominantly associated with 43S preribosomes, and it has been shown to interact with the SSU processome protein Utp13 in a yeast two-hybrid assay (21). Taken together, these results strongly suggest that Fap7 has a direct role in pre-rRNA processing.

In this work, we demonstrate that Fap7 is strictly required for cleavage at site D but not at any other processing steps, indicating that it has a role in the final cleavage step that generates the mature SSU. Strikingly, genetic depletion of Fap7 results in the accumulation of unusually high levels of 20S pre-rRNA in the cytoplasm. In contrast to other known nonribosomal proteins whose depletion causes accumulation of

* Corresponding author. Mailing address: Yale University School of Medicine, Department of Molecular Biophysics and Biochemistry, 333 Cedar Street, SHM C-114, New Haven, CT 06520-8024. Phone: (203) 785-4618. Fax: (203) 785-6404. E-mail: susan.baserga@yale.edu.

† Supplemental material for this article may be found at http://mcb.asm.org/.

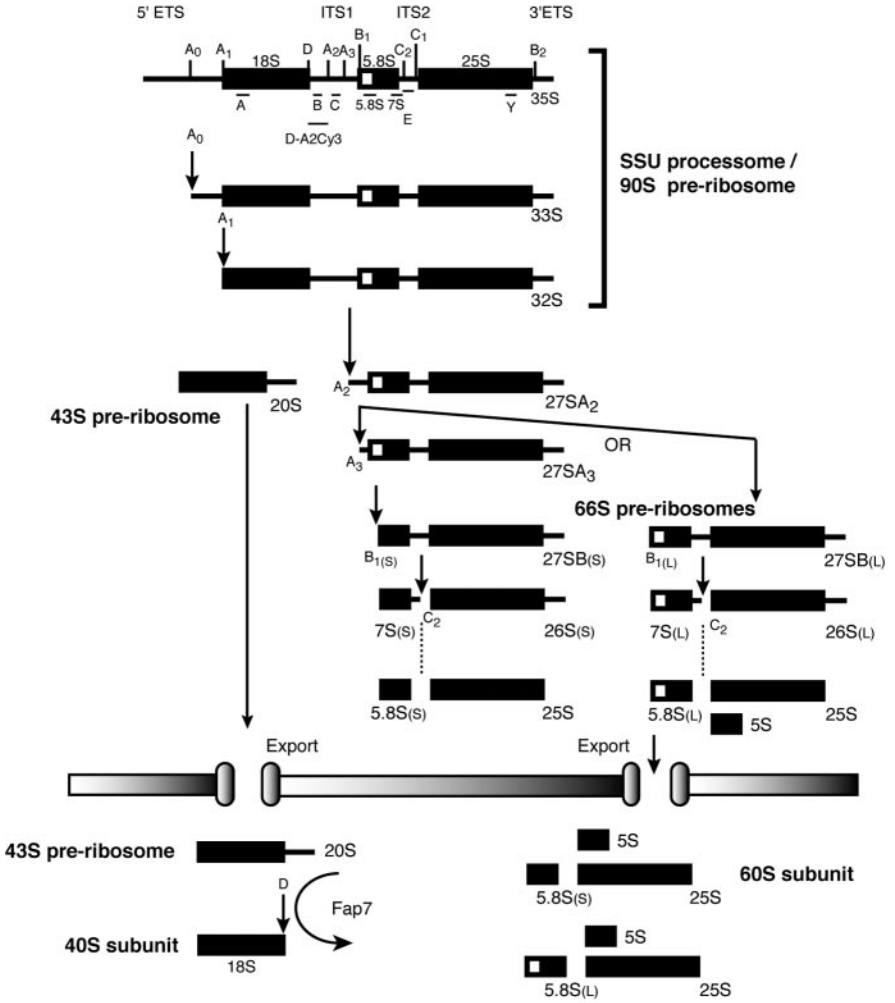

FIG. 1. Schematic representation of the pre-rRNA-processing pathway in the yeast *Saccharomyces cerevisiae*. RNA polymerase I transcribes the 35S pre-rRNA, which contains the mature rRNA sequences (18S, 5.8S, and 25S), ITS, and ETS. The 5.85 rRNA has both short (S) and long (L) forms. The 5S rRNA is transcribed by RNA polymerase III and joins 66S preribosomes in the nucleus. The positions of the oligonucleotides used in this study are indicated.

the 20S pre-rRNA, Fap7 is probably not a structural component of 43S preribosomes but most likely transiently interacts with these complexes by directly binding Rps14, placing Fap7 in close proximity to the D cleavage site. In agreement with its predicted NTPase activity, we show that conserved residues in the putative Walker A and Walker B motifs which are predicted to be involved in nucleotide binding are important for Fap7 function in vivo. Collectively, our results support a model in which processing of the 20S pre-rRNA at site D in the cytoplasm requires a transient interaction between Fap7 and Rps14 within the 43S preribosome.

MATERIALS AND METHODS

Yeast strains and media. YPH499 (*mat***a** *ura3-52 lys2-80 ade2-101 trp1-Δ63 his3-Δ200 leu2-Δ1*) was the parental strain for the strains constructed here. Strains carrying galactose-inducible, triple-hemagglutinin (HA)-tagged genes (Kan^r marker) were generated as described previously (29). Strains expressing TAP carboxyl-tagged proteins (*Kluyveromyces lactis TRP* marker) were generated as described previously (37). Unless otherwise noted, strains were grown in YPD (1% yeast extract, 2% peptone, 2% dextrose) at 30°C. *GAL*::*3HA* strains were grown in YPG/R (1% yeast extract, 2% peptone, 2% galactose, 2% raffinose) until shifted to YPD. Strains carrying p415GPD::*FAP7* plasmids (*CEN* origin of replication and *LEU* marker) were grown at 30°C in synthetic complete minus leucine (Clontech) supplemented with 2% dextrose or with 2% galactose and 2% raffinose.

DNA manipulations. The *FAP7* allele was PCR amplified from yeast genomic DNA and cloned into the p415GPD vector (CEN plasmid) using BamHI and XhoI restriction sites. Mutants were generated using a QuikChange site-directed mutagenesis kit (Stratagene) according to the manufacturer's procedures. To overexpress Fap7 in bacteria, *FAP7* was amplified by PCR from yeast genomic DNA and cloned into pET28a using BamHI and NotI restriction sites. Following PCR amplification, *RPS14B* wild-type and *rps14B R134A* alleles were cloned into pGEX6P using EcoRI and NotI restriction sites. To overexpress and purify GST-YOR287C, the YOR287C allele was amplified by PCR from yeast genomic DNA and cloned into pGEX6P-2 using BamHI and EcoRI restriction sites. All constructs were verified by automated DNA sequencing (W.M. Keck DNA-sequencing facility at Yale).

RNA manipulations. For the depletion experiments shown in Fig. 2, cells were depleted for a maximum of 10 or 24 h, depending on when the rate of growth changed. Exponentially growing cells were harvested 0, 5, 10, and 24 h after the shift to YPD. For the detection of high-molecular-weight RNA species, 10 μg of total RNA was resolved on formaldehyde-1.25% agarose gels as described previously (5). To detect small RNAs, 10 μg of total RNA was separated on 8% polyacrylamide-8 M urea gels. RNA extractions, Northern blotting, primer extension, and pulse-chase analyses with [5,6-^{3}H]uracil were carried out as de-

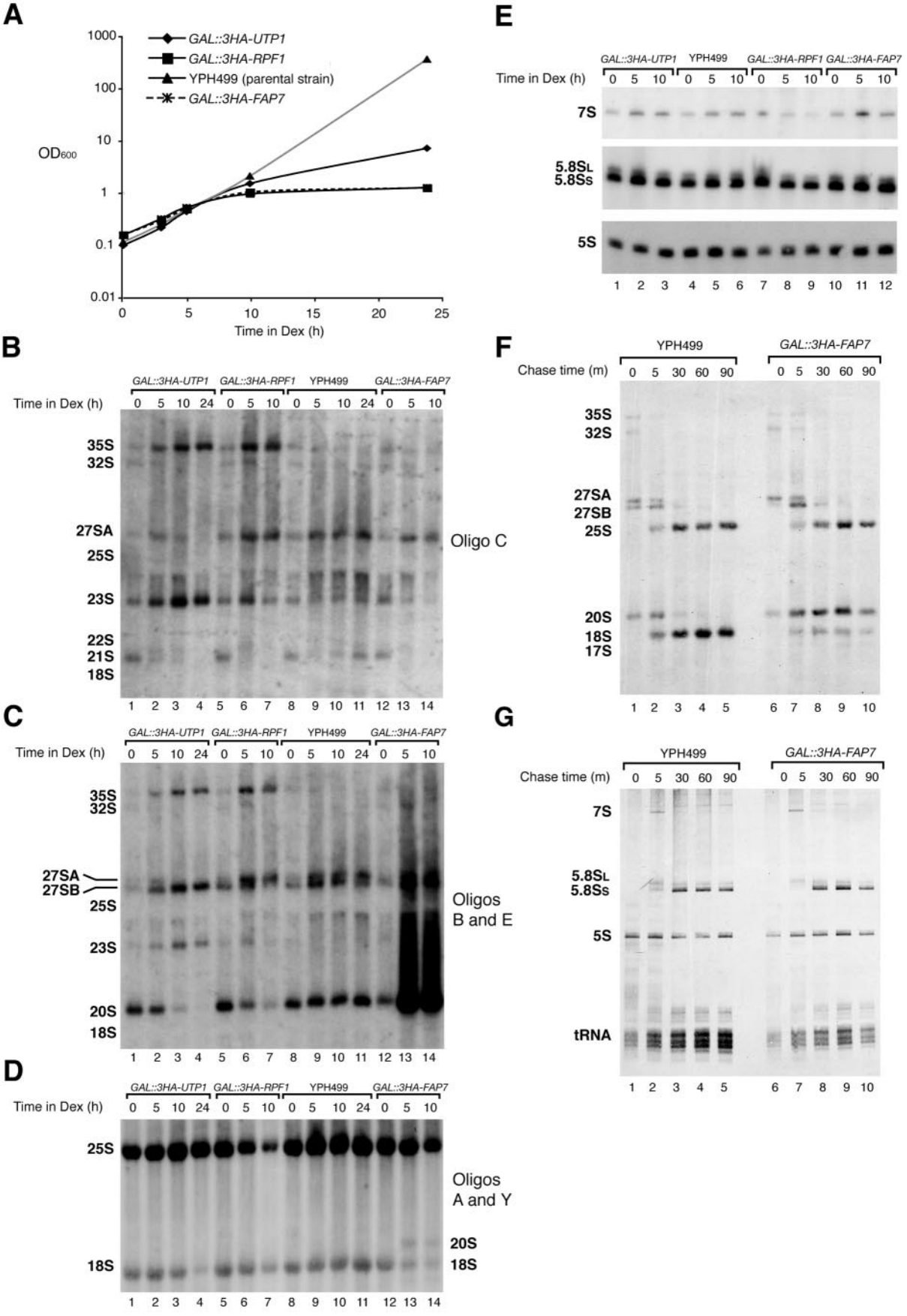
A
GAL::3HA-UTP1
GAL::3HA-RPF1
YPH499 (parental strain)
GAL::3HA-FAP7
OD600
Time in Dex (h)
B
Time in Dex (h)
35S
32S
27SA
25S
23S
22S
21S
18S
Oligo C
C
Time in Dex (h)
35S
32S
27SA
27SB
25S
23S
20S
18S
Oligos B and E
D
Time in Dex (h)
25S
18S
Oligos A and Y
20S
18S
E
Time in Dex (h)
7S
5.8SL
5.8Ss
5S
F
Chase time (m)
35S
32S
27SA
27SB
25S
20S
18S
17S
G
Chase time (m)
7S
5.8SL
5.8Ss
5S
tRNA

scribed previously (5). Oligonucleotides used for Northern analysis were as follows: A (5′-CATGGCTTAATCTTTGAGAC-3′), B (5′-GCTCTTTGCTCT TGCC-3′), C (5′-ATGAAAACTCCACAGTG-3′), E (5′-GGCCAGCAATTT CAAGT-3′), and Y (5′-GCCCGTTCCCTTGGCTGTG-3′). Small RNA oligonucleotide probes were as follows: 5.8S (5′-TTTCGCTGCGTT-3′), 7S (5′-TGA GAAGGAAATGACGCT-3′), and 5S (5′-CTACTCGGTCAGGCTC-3′).

Expression and purification of recombinant proteins. All fusion proteins were expressed in *Escherichia coli* BL21(DE3). Cells were grown in Luria broth (LB) at 37°C with either kanamycin (pET28a) or ampicillin (pGEX) to an optical density at 600 nm (OD_{600}) of 0.4 to 0.5 and then grown for an additional 2 hours at 17°C. Protein expression was induced with 1 mM isopropyl-β-D-thiogalactoside (IPTG) for 16 to 20 h at 17°C. Cells were harvested by centrifugation, and pellets were resuspended in 5 to 8 volumes of breaking buffer (150 mM KCl, 50 mM Tris-HCl [pH 7.4], 10% sucrose, 0.5 mM EDTA, 1 mM β-mercaptoethanol, 0.01% Igepal [Sigma]) containing a protease inhibitor cocktail (10 μg/ml aprotinin, 10 μg/ml leupeptin, 10 μg/ml chymostatin, 10 μg/ml pepstatin, 1.3 mM benzamidine; Sigma) and disrupted using a French press. Extracts were clarified by ultracentrifugation at 100,000 × *g* for 1 h. To purify recombinant six-histidine-tagged Fap7 protein, clarified extracts were incubated with Ni-nitrilotriacetic acid beads (1 ml beads/5 g of cell pellet; QIAGEN) for 1 h at 4°C. After being poured into a column, beads were subsequently washed with 10 bead volumes of K1000 buffer (20 mM $KHPO_4$ [pH 7.4], 1 M KCl, 0.5 mM EDTA, 10% glycerol, 1 mM β-mercaptoethanol, 0.01% Igepal) and with 10 bead volumes of K300 (like K1000 but with 300 mM KCl instead of 1 M) containing 50 mM imidazole. Proteins were eluted with 5 bead volumes of K300 containing 500 mM imidazole. Eluates containing nearly homogenous recombinant protein were pooled and dialyzed overnight in K150 buffer containing 20% glycerol and stored at −80°C in small fractions. This procedure yielded 5 to 10 mg/ml protein and ~25 mg of protein per liter culture, which was approximately 90%-pure recombinant protein, as judged by sodium dodecyl sulfate-polyacrylamide gel electrophoresis (SDS-PAGE) and Coomassie brilliant blue staining. To purify the glutathione *S*-transferase (GST)-Rps14B wild-type and R134A proteins, the conductivity of extracts prepared from 10 g of cells was adjusted to that of 100 mM KCl and passed sequentially over 10-ml Q and SP Sepharose columns preequilibrated with K100 buffer (like K1000 but with 100 mM KCl instead of 1 M). The SP Sepharose column was washed extensively with K100, and bound proteins were eluted with a 30-ml linear salt gradient (100 mM to 1,000 mM KCl) prepared in K buffer (20 mM $KHPO_4$ [pH 7.4], 0.5 mM EDTA, 10% glycerol, 1 mM β-mercaptoethanol, 0.01% Igepal). Fractions containing GST-Rps14B proteins were pooled, and the conductivity was adjusted to that of 300 mM KCl. This mixture was then incubated with 2 ml of glutathione-Sepharose beads (Amersham) for 1 hour at 4°C. After the beads were washed extensively with K150 buffer, proteins were eluted with K150 containing 20 mM reduced glutathione (USB). Eluates containing nearly homogenous recombinant protein were pooled and dialyzed overnight in K150 buffer containing 20% glycerol and stored at −80°C in small aliquots. Recombinant GST-YOR287C was purified as described for GST-Rps14 except that the Q Sepharose step was omitted.

Protein-protein interactions. Ten μg of bovine serum albumin (BSA; Sigma) and six-histidine-tagged Fap7 was incubated with 10 μg of GST, 5 μg of GST-YOR287C, 5 μg of GST-Rps14B or 5 μg GST-Rps14B R134A protein in K150 buffer in a final volume of 30 μl. After 1 h of incubation on ice, 190 μl of K150 was added to the mixtures, 20 μl was removed for analysis (10% input), and the remainder was incubated with 10 μl of glutathione-Sepharose beads (Amersham) for 1 hour on ice with regular agitation. Beads were spun down by centrifugation, and 20 μl of the supernatant was subsequently removed for analysis (10% supernatant). The beads were washed three times with 1 ml of ice-cold K150. Bound proteins were extracted by boiling the beads in SDS-PAGE loading dye and resolved by 10% SDS-PAGE. Proteins were visualized by Coomassie brilliant blue staining.

Sucrose density gradient centrifugation. Fap7 depletion strains expressing TAP-tagged Rio2, Tsr1, or Nob1 were grown in YPG/R to an OD_{600} of 0.5, harvested, washed with ice-cold phosphate-buffered saline (PBS), shifted to YPD at an OD_{600} of 0.1, and grown for 5 h at 30°C to deplete Fap7. Cells (50 ml; OD_{600} of ~0.5) were collected by centrifugation, washed with ice-cold PBS, and resuspended in 600 μl of lysis buffer (100 mM HEPES-KOH [pH 7.4], 10 mM KCl, 1 mM EGTA, 2.5 mM $MgCl_2$, 0.1% Igepal, 1 mM dithiothreitol) with the protease inhibitor cocktail (see above) and 10 mM vanadyl ribonucleoside complex (VRC; USB). Whole-cell extracts were prepared by vortexing the suspension 5 times for 45 seconds with acid-treated glass beads (0.5 mm) at 4°C. Extracts were clarified by centrifugation at 10,000 × *g*, and 500 μl of extract was layered on a 12-ml 10% to 50% sucrose gradient (wt/vol) prepared in gradient buffer (10 mM HEPES-KOH [pH 7.4], 10 mM KCl, 1 mM EGTA, 2.5 mM $MgCl_2$, 0.1% Igepal). Gradients were centrifuged for 7 h in an SW41 rotor at 39,000 rpm. Twenty fractions (600 μl) were manually collected. For the profiles shown in Fig. 3A and B, fractions were collected using an Isco gradient fraction collector, and protein content was monitored with UV at A_{254} nm. RNA from each fraction was isolated by phenol-chloroform-isoamyl alcohol extraction and ethanol precipitation and resolved on formaldehyde-1.25% agarose gels, which was followed by Northern blot analysis. Proteins were trichloracetic acid precipitated prior to separation by 10% SDS-PAGE. Western blot analysis was performed as described previously (12). Antibodies used (PAP [Sigma], 17C12 anti-HA monoclonal) have been described elsewhere (12).

Immunoprecipitations. *GAL*::*3HA-FAP7* strains were grown to an OD_{600} of 0.5, centrifuged, washed with PBS, diluted in YPD to an OD_{600} of 0.1, and grown for 5 h to deplete Fap7. Fifty milliliters of cells grown at an OD_{600} of ~0.5 were collected by centrifugation, washed with ice-cold PBS, and resuspended in 600 μl of IPP150 plus VRC (50 mM Tris [pH 7.5], 150 mM KCl, 2.5 mM $MgCl_2$, 0.1% Igepal, 1 mM dithiothreitol) containing the protease inhibitor cocktail and 10 mM VRC. Extracts were prepared using the glass bead method described above. RNA extracted from 25 μl was used as 5% input. Five hundred μl of extract was incubated with 10 μl immunoglobulin G-Sepharose beads (Amersham) for 1 hour at 4°C. Beads were washed three times with 500 μl ice-cold lysis buffer and twice with 500 μl ice-cold IPP150 without VRC and protease inhibitors. RNA extraction and analysis was performed as described above. Oligonucleotide B was used to detect the 20S pre-rRNA.

FISH experiments. The oligonucleotide used for fluorescent in situ hybridization (FISH) was D-A2 (5′-GCTGGACTCTCCATCTCTTGTCTTCTTGCC CAGTAAAAGCTCTTTGCTCT-3′). Cy3 labeling was performed using a Cy3-ULS labeling kit (Amersham) according to the manufacturer's procedures. Cells were fixed and mounted on coverslips as described previously (4). FISH was performed as described on the Singer Lab protocol page (http://www.singerlab.org/protocols). Fixed cells were washed twice with PBS, and the cells were covered in 20 μl of hybridization buffer (10 mM $NaPO_4$ [pH 7.0], 40% formamide, 4× SSC [1× SSC is 0.15 M NaCl plus 0.015 M sodium citrate], 10% dextran sulfate, 1× Denhardt's solution, 100 mg/ml denatured salmon sperm DNA, 1 mg/ml *E. coli* tRNA, 2 mg/ml BSA) for 1 hour at 37°C. Cells were hybridized overnight at 37°C in 40 μl of hybridization buffer with 100 ng of Cy3-labeled D-A2 probe. Cells were washed twice for 30 min with 2× SSC and 50% formamide at 37°C and once with PBS for 5 min. Cells were incubated with TOPRO3 dye (1:1,000 in PBS; Molecular Probes) for 5 min, which was followed

FIG. 2. Fap7 is required for processing of the 20S pre-rRNA at site D. (A) Growth rates of the *UTP1*, *RPF1*, and *FAP7* depletion strains as well as that of the parental strain YPH499 in dextrose medium (YPD [Dex]). Growth was monitored for 24 h in YPD. (B to E) Northern analysis indicating that depletion of Fap7 blocks processing of the 20S pre-rRNA at site D but does not affect processing at A_0, A_1, or A_2. Exponentially growing depletion strains (*GAL*::*3HA-UTP1*, *GAL*::*3HA-RPF1*, and *GAL*::*3HA-FAP7*) and the parental strain (YPH499) were shifted from YPG/R to YPD, and cells were grown for 10 to 24 h. RNA was extracted from cells harvested at the indicated times, and equal amounts of RNA were resolved by 1.25% denaturing agarose gels (panels B to D) or 8% polyacrylamide-8 M urea gel (panel E), transferred to Hybond N^+ membranes, and hybridized with several radiolabeled oligonucleotides (oligos) (panels B to D; indicated at the side of each panel). The positions of the various pre-rRNA species on the membranes are indicated on the left of each panel. Time points that were analyzed (h) and the strains used in the experiments are indicated on top of each panel. (F and G) Metabolic labeling indicating that depletion of Fap7 specifically inhibits processing at site D. The *GAL*::*3HA-FAP7* and parental (YPH499) strains, both carrying a plasmid with a URA marker, were grown in galactose medium lacking uracil (SG/R-URA) to exponential phase and shifted to the nonpermissive dextrose medium (SD-URA), and after 5 h the cells were labeled with [5,6-^{3}H]uracil for 2 minutes and then chased with an excess of cold uracil. Total RNA extracted from cells harvested at the indicated time points (in minutes) was analyzed by 1.2% denaturing agarose gels (panel F) and 8% polyacrylamide-8 M urea gel (panel G). The positions of the rRNA, pre-rRNA species, and tRNA are indicated on the left of each panel.

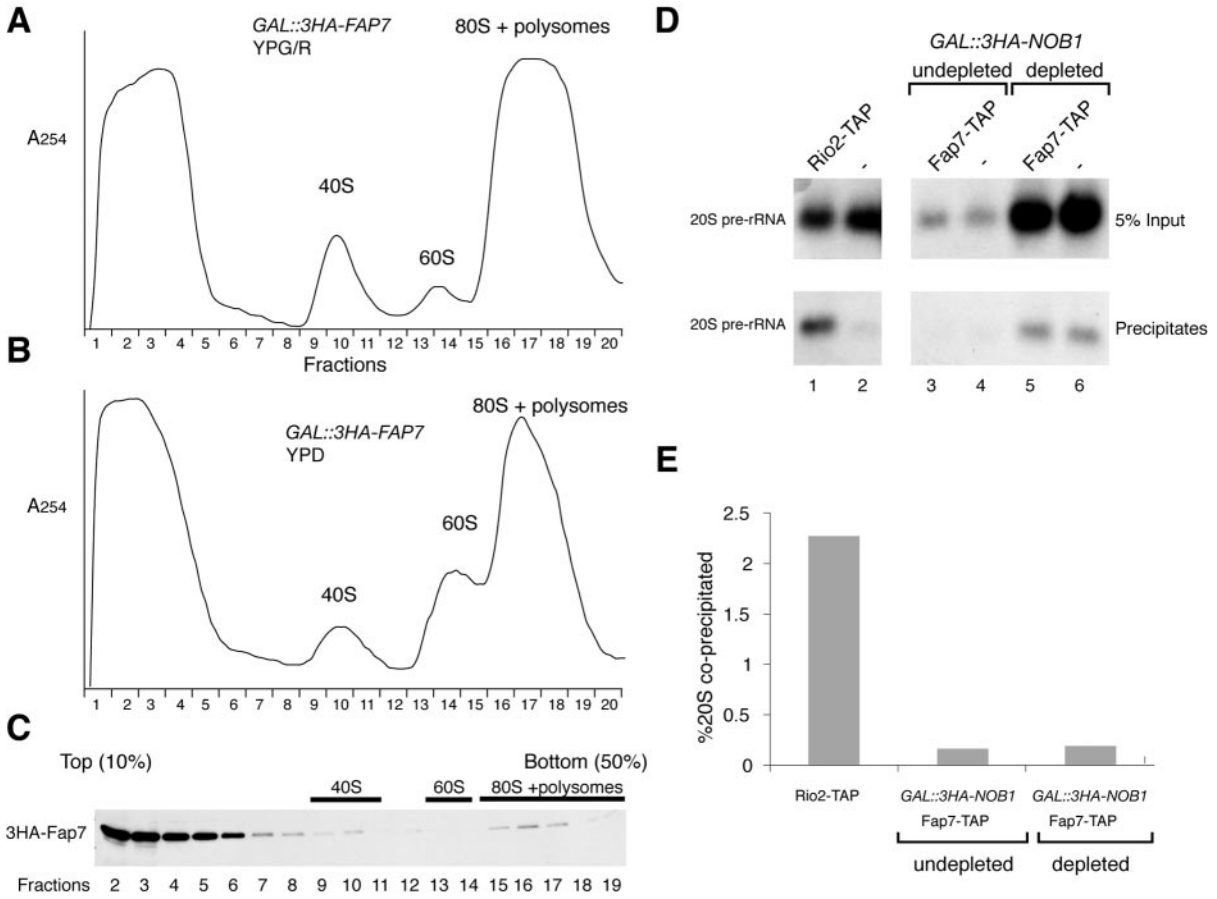

FIG. 3. Fap7 is essential for 40S subunit synthesis but is not stably associated with 20S pre-rRNA and preribosomes. (A and B) Fap7 is required for the production of 40S ribosomal subunits. Extracts from *GAL*::*3HA-FAP7* cells grown either in the permissive galactose medium only (panel A; YPG/R) or grown in the permissive medium and shifted to the nonpermissive dextrose medium for 5 h (panel B; YPD) were fractionated by 10% to 50% sucrose gradient centrifugation. The positions of ribosomal subunits, 80S ribosomes, and polysomes in the gradients were determined by measurements of absorption at 254 nm. (C) Sedimentation of 3HA-Fap7 in a 10% to 50% sucrose gradient. Extracts prepared from *GAL*::*3HA-FAP7* cells grown in YPG/R were fractionated by 10% to 50% sucrose gradient centrifugation, and the sedimentation of 3HA-Fap7 in the gradient was determined by Western blot analysis. (D and E) Fap7-TAP does not coprecipitate the 20S pre-rRNA even when 20S pre-rRNA levels are increased by depleting Nob1. Strains (*RIO2-TAP*, *GAL*::*3HA-NOB1*, and *FAP7-TAP*) were grown in YPG/R to mid-log phase. The *GAL*::*3HA-NOB1* and *FAP7-TAP* strains were subsequently shifted to YPD and grown for 6 h to deplete Nob1 (depleted). Rio2-TAP and Fap7-TAP were immunoprecipitated from extracts using immunoglobulin G-Sepharose beads. RNA extracted from 5 percent of the starting material and coprecipitated RNAs were resolved on 1.25% denaturing agarose gels. The 20S pre-rRNA was detected using oligonucleotide B. As negative controls, strains without TAP tags were used (lanes 2, 4 and 6 [−]). (E) Quantification of the results shown in panel D. The percentage of coprecipitated 20S pre-rRNA was determined using values generated from phosphorimager scans.

by two 5-min washes with PBS. Slides were mounted in 90% glycerol, PBS, and 1 mg/ml *p*-phenylendiamine. Pictures were taken using an inverted Zeiss 510 Meta confocal microscope and modified using Adobe Photoshop CS.

RESULTS

Fap7 is strictly required for cleavage of the 20S pre-rRNA at site D. Although Peng et al. have recently shown that Fap7 is required for processing of the 20S pre-rRNA at site D by microarray and by Northern blot analysis, the effect of Fap7 depletion on other pre-rRNA-processing steps was not investigated (35). Therefore, to gain more insight into the role of Fap7 in ribosome biogenesis, we reexamined the effect of its in vivo depletion on pre-rRNA processing. Since *FAP7* is essential for growth (23), we constructed a conditional allele in which a chromosomal N-terminal triple-HA-tagged *FAP7* allele was placed under the control of a galactose-inducible/dextrose-repressible promoter (*GAL*::*3HA-FAP7*). We also tested a number of strains that were not predicted to have cleavage defects at site D as controls. Results with the *GAL*::*3HA-UTP1* strain demonstrated that Utp1 is required for cleavage at the A_0, A_1, and A_2 sites necessary for 18S rRNA synthesis (4), while the *GAL*::*3HA-RPF1* strain was used to show that Rpf1 is required for pre-25S rRNA processing (48). YPH499 is the parental strain. Cells were grown in galactose-containing media (YPG/R) to mid-log phase and shifted to dextrose media (YPD), and growth was monitored for 24 h. In the first 5 h following transfer to YPD, the *GAL*::*3HA-FAP7* and *GAL*::*3HA-RPF1* strains grew at a rate similar to that of the parental strain (YPH499), but growth steadily decreased after approximately 7 hours and plateaued after 10 h of depletion (Fig. 2A). In contrast, growth of the *GAL*::*3HA-UTP1* strain was

comparable to that of the parental strain until approximately 10 h in YPD, after which growth slowed progressively.

To examine the pre-rRNA-processing defects in Fap7-depleted cells, we performed Northern blot analyses on RNA extracted from cells harvested 0, 5, 10, and 24 h after the shift to YPD. Blots were hybridized with probes specific for pre-rRNAs or mature rRNAs (Fig. 1 and 2). Strikingly, even at just 5 h after the shift to YPD (approximately two doublings), Fap7 depletion resulted in 20S pre-rRNA accumulation and a marked decrease in 18S rRNA levels (Fig. 2C and D, lanes 12 to 14). So much 20S pre-rRNA accumulated that levels were approximately equal to that of the mature 18S rRNA. In contrast, relative to Utp1- and Rpf1-depleted cells, Fap7-depleted cells did not have noticeable defects in processing of the 35S pre-rRNA at sites A_0, A_1, and A_2 or of the pre-LSU rRNAs, as illustrated by the unaltered levels of 35S, 27SA, 27SB, and 23S pre-rRNAs and of the mature 25S rRNA after the shift to YPD (Fig. 2A to D, lanes 12 to 14). Notably, we observed in all strains a modest increase of most pre-rRNAs 5 hours after the shift to YPD, which is likely due to the nutritional upshift from the switch to dextrose-containing medium. In addition, no noticeable defects in the processing of 7S pre-rRNA and synthesis of 5.8S and 5S rRNAs were observed (Fig. 2E, lanes 10 to 12), indicating that processing in ITS2 was normal. Consistent with previously published work, Rpf1 depletion resulted in reduced accumulation of the 7S pre-rRNA (48).

To substantiate these results, we performed a metabolic labeling experiment to monitor the synthesis and processing of pre-rRNA in vivo upon Fap7 depletion. The *GAL*::*3HA-FAP7* and parent (YPH499) strains were grown to mid-log phase in YPG/R and then shifted to YPD. After 5 h, the cells were labeled with [5,6-^{3}H]uracil and chased by adding an excess of cold uracil. rRNA production was monitored at 0, 5, 30, 60, and 90 min after labeling. Consistent with the results from steady-state RNA analysis, Fap7-depleted cells accumulated high levels of 20S pre-rRNA and synthesized very little mature 18S rRNA (Fig. 2F, lanes 6 to 10). Fap7-depleted cells showed no delay in processing the 35S and 32S pre-rRNAs to 20S and 27SA pre-rRNAs, demonstrating that processing at sites A_0, A_1, and A_2 was unaffected. Similarly, no noticeable defects in pre-LSU rRNA processing were observed (Fig. 2F and G). Longer exposures of the blot also revealed a band migrating faster than that of the 18S rRNA; this band may represent the 17S rRNA (22).

Taken together, our results suggest that Fap7 is required exclusively for cleavage of the 20S pre-rRNA at site D, which is essential for the synthesis of the mature 18S rRNA.

Fap7 is essential for SSU synthesis but is not a structural component of 43S preribosomes. We examined the result from depletion of Fap7 on the production of both ribosomal subunits and on the 80S ribosome. Extracts prepared from *GAL*::*3HA-FAP7* cells grown in YPG/R only (Fig. 3A) or in YPG/R and then in YPD for 5 h (depleted cells in Fig. 3B) were fractionated by 10% to 50% sucrose gradient centrifugation, and the distribution of ribosomal components was examined by measurements of absorption at 254 nm. Compared to the control cells (Fig. 3A), Fap7-depleted cells contained fewer 40S ribosomal subunits and increased numbers of free 60S subunits, consistent with a role for it in SSU maturation.

Notably, in the permissive YPG/R medium, the levels of free SSU in the *GAL*::*3HA-FAP7* strain were consistently higher than the levels of free LSU, which is somewhat atypical. It is possible that this is the result of overexpression of Fap7 from the *GAL* promoter.

All of the known proteins required for processing of 20S pre-rRNA, including Enp1, Rrp12, Tsr1, Rio1, Rio2, and the putative endonuclease Nob1, cosediment with the SSU in density gradients, are associated with 43S preribosomes, and interact with the 20S pre-rRNA (6, 15, 34, 39, 44, 45). Previously, Fap7 copurified with the 43S-associated protein Enp1-TAP by tandem affinity purification (14). Therefore, we reasoned that Fap7 likely interacts with 43S preribosomes. Much to our surprise, Western blot analysis of sucrose gradient fractions demonstrated that the bulk of the Fap7 protein was present in small complexes or as free protein, while very little was detected in regions corresponding to 40S ribosomal subunits. Similarly, Fap7 TAP tagged at the C terminus was also found sedimenting predominantly as free protein (see Fig. S1 in the supplemental material). However, a small amount of Fap7 sedimented at 80S (Fig. 3C). In addition, the results of immunoprecipitation experiments show that, unlike Rio2-TAP, Fap7-TAP did not coprecipitate significant amounts of 20S pre-rRNA (Fig. 3D, lanes 1 and 3, and E). These results suggest that only a very small amount of Fap7 associates with 43S preribosomes. However, we cannot exclude the possibility that the association of Fap7 with 43S preribosomes may have been lost during the preparation of the extracts or during the course of the experiments.

Genetic depletion of Nob1 results in accumulation of the 20S pre-rRNA and 43S preribosomes (6), similar to the result we have observed for Fap7. We asked whether interactions between Fap7 and 43S preribosomes could be artificially stabilized if we increased the levels of 20S pre-rRNA and 43S preribosomes by depleting Nob1. For this purpose, *NOB1* was placed under the control of the galactose-inducible/dextrose-repressible promoter in a strain expressing a TAP-tagged Fap7 protein. Disappointingly, even though the level of 20S pre-rRNA in Nob1-depleted cells was 5- to 10-fold higher than that in normally growing cells, we still could not detect significant association of Fap7-TAP with 20S pre-rRNA (Fig. 3D, lanes 3 and 5, and E). In addition, the distribution of Fap7 in sucrose gradients did not change when Nob1 was depleted (data not shown).

Thus, our results suggest that while Fap7 is essential for the production of the SSU via a requirement for site D cleavage, it is likely not a structural component of 43S preribosomes.

Fap7 is required for pre-rRNA processing in the cytoplasm. Fap7 is present in both the nucleus and the cytoplasm (20, 23), and thus there are two possible cellular locations for Fap7 function. Fap7 could be involved in the export of 43S preribosomes, which contain the 20S pre-rRNA, from the nucleus to the cytoplasm. If so, depletion of Fap7 would cause nuclear accumulation of the 20S pre-rRNA. Alternatively, Fap7 could be directly involved in cleavage of the 20S pre-rRNA within 43S preribosomes at site D in the cytoplasm. In this case, its depletion would lead to accumulation of 20S pre-rRNA in the cytoplasm. To differentiate between these possibilities, we performed FISH experiments using a Cy3-labeled probe that hybridizes between cleavage sites D and A_2 (D-A2Cy3 in Fig. 1 and 4A) and detects the 35S, 33S, 32S, 23S, and 20S transcripts (Fig. 1). FISH was performed on YPH499 cells grown to mid-

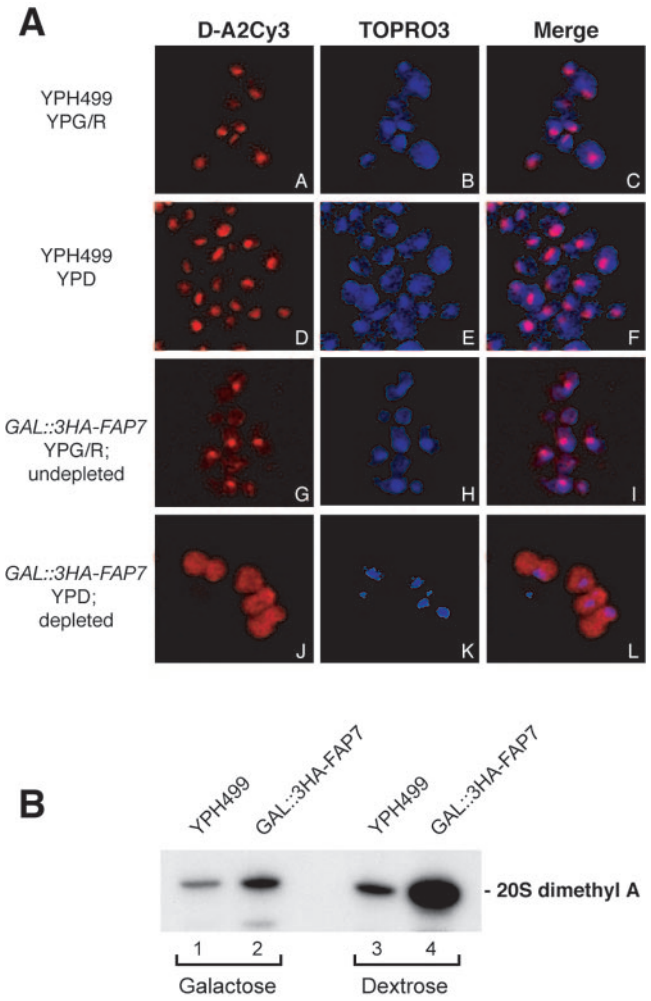

FIG. 4. (A) Depletion of Fap7 causes accumulation of 20S pre-rRNA in the cytoplasm. FISH was performed on strains (YPH499 and *GAL*::*3HA-FAP7*) grown in galactose medium (YPG/R) (panels A to C and G to I) or dextrose medium (YPD) (panels D to F and J to L). TOPRO3 dye was used to stain nuclei (panels B, E, H, and K). FISH was performed using a Cy3-labeled D-A2 oligonucleotide that hybridizes to the 35S to 32S and 20S pre-rRNAs. (B) Fap7 depletion does not prevent Dim1-mediated dimethylation of the 20S pre-rRNA. Primer extension analysis on total RNA extracted from strains, indicated on top of the figure, grown in galactose-containing medium (YPG/R) only or grown in galactose-containing medium and shifted to dextrose-containing medium (YPD) for 5 hours. RNA was resolved on a 6% polyacrylamide-8 M urea gel and subjected to autoradiography.

log phase in YPG/R or YPD (Fig. 4A, panels A to F) and on the *GAL*::*3HA-FAP7* strain either grown in YPG/R only (*GAL*::*3HA-FAP7* undepleted cells in Fig. 4A, panels G to I) or grown also in YPD for 5 hours to deplete Fap7 (*GAL*::*3HA-FAP7* depleted cells in Fig. 4A, panels J to L). TOPRO3 dye was used to stain the cell nuclei. In the parental strain YPH499, the D-A2Cy3 probe predominantly stained a crescent-shaped structure in the nucleus, which likely represents the nucleolus (Fig. 4A, panels A and D). Also, faint staining was detected in the cytoplasm. This strong nucleolar signal results from hybridization of the probe with the anticipated pre-rRNAs. Importantly, the fluorescence intensity and the staining pattern were not affected by switching the carbon source (Fig. 4A, panels A to F). FISH with *GAL*::*3HA-FAP7* cells grown in the permissive YPG/R medium showed a similar staining pattern (Fig. 4A, panels G to I). In Fap7-depleted cells, the fluorescence was dispersed throughout the entire cell, with the highest concentration in the cytoplasm (Fig. 4A, panels J to L). Since the 20S pre-rRNA is the only pre-rRNA that is exported, this is a very strong indication that these cells accumulate the 20S pre-rRNA in the cytoplasm. Furthermore, primer extension analysis on RNA extracted from Fap7-depleted cells showed that the accumulated 20S pre-rRNA was efficiently dimethylated at the Dim1 methylation site near the 3′ end of the 18S rRNA, a modification that takes place in the cytoplasm (Fig. 4B, lane 4) (3, 25, 26). Thus, these results strongly suggest that Fap7 is not involved in nuclear export of the 43S preribosomes but is required for cleavage of the 20S pre-rRNA at site D in the cytoplasm.

Depletion of Fap7 results in the accumulation of smaller 43S preribosomes. We determined whether the block in 20S pre-rRNA processing in Fap7-depleted cells was related to defects in the assembly of 43S preribosomes. We constructed *GAL*::*3HA-FAP7* strains in which known 43S preribosome components were fused to the TAP tag at their carboxy termini (Rio2-TAP, Nob1-TAP, and Tsr1-TAP in Fig. 5A). Sucrose gradient analyses revealed that when these strains are grown in YPG/R, the distribution of Rio2-TAP, Nob1-TAP, and Tsr1-TAP in the gradients is almost identical to that described previously (6, 39, 44). In most cases, the bulk of each of the proteins sedimented around 40S, likely corresponding to the 43S preribosomes. Nob1-TAP was also detected at 80S, and Rio2-TAP was found in small complexes or as free protein. Remarkably, in the absence of Fap7, the distribution of Rio2-TAP and Tsr1-TAP in the gradients changed markedly (depleted cells in Fig. 5A). In Fap7-depleted cells, some Rio2-TAP and Tsr1-TAP shifted to larger complexes (80S). Nob1-TAP, Rio2-TAP, and Tsr1-TAP were also detected around 40S in Fap7-depleted cells; relative to that of the control cells, however, this peak shifted to smaller complexes by only one fraction (Fig. 5A, compare depleted and undepleted cells). These smaller complexes may represent incomplete, unstable, or partially degraded 43S preribosomes (see also below).

We also analyzed the distributions of the 20S pre-rRNA and the mature 18S and 25S rRNAs in the gradient fractions by Northern blot analysis (Fig. 5B). In Fap7-depleted cells, Rio2, Nob1, and Tsr1 proteins cosediment with the 20S pre-rRNA, suggesting that the smaller 43S complexes and the 80S-sized complexes contain the 20S pre-rRNA. Notably, in contrast to what was found in normally growing cells, almost all of Rio2 was found associated with ~40S- and ~80S-sized complexes in Fap7-depleted cells. In addition, we detected in Fap7-depleted cells the 17S rRNA cosedimenting with the 20S pre-rRNA and the 18S rRNA in fractions corresponding to 40S but not to 80S. In the undepleted cells, the 20S pre-rRNA was detectable only in the 40S-sized fractions (undepleted cells in Fig. 5B). Because the 17S rRNA is a degradation product (22), it is very likely that a fraction of the accumulated 43S preribosomes in Fap7-depleted cells is unstable and/or partially degraded, which may explain why we observed slightly smaller 43S preribosomes accumulating in Fap7-depleted cells.

Collectively, while Fap7 depletion leads to accumulation of

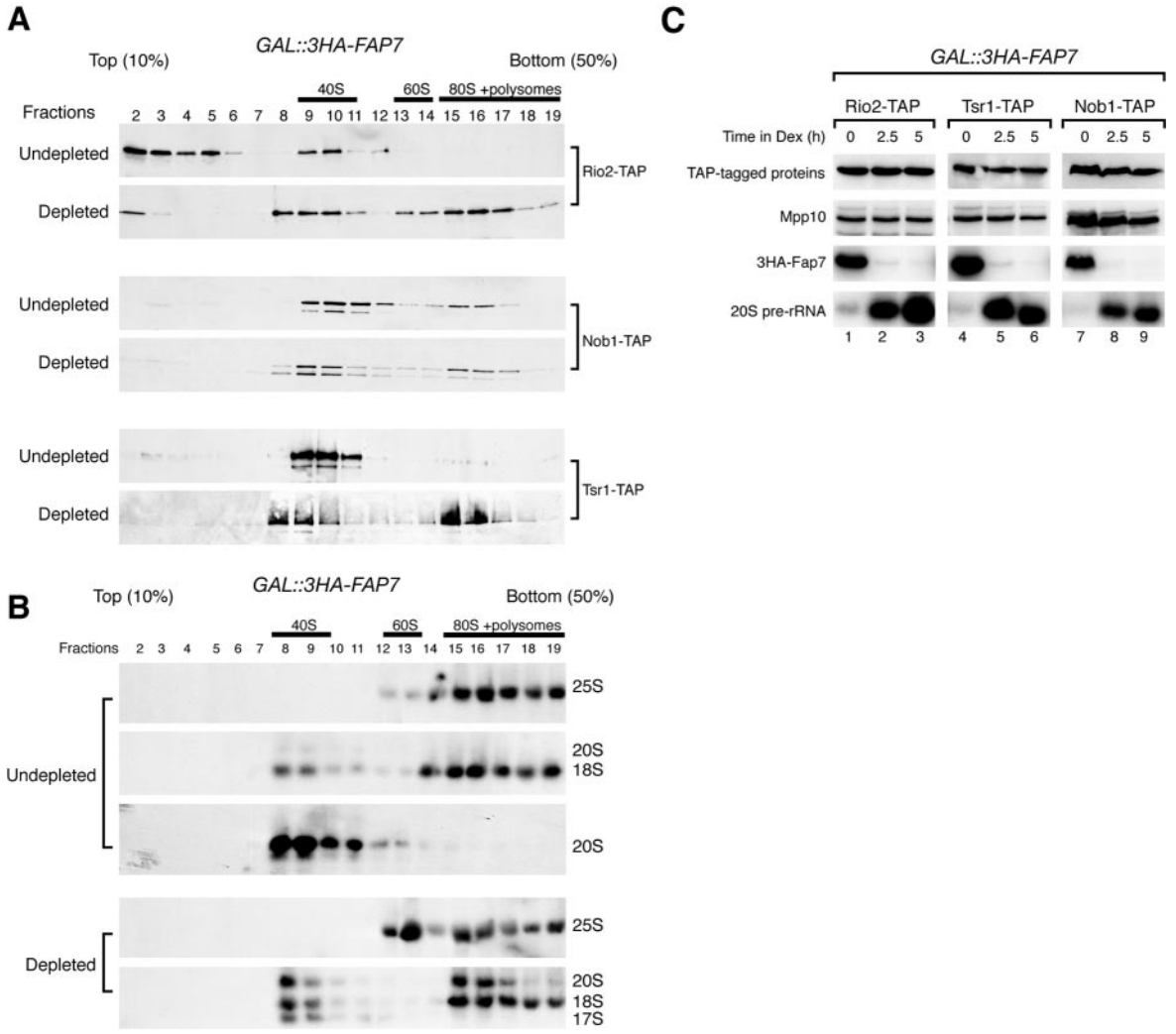

FIG. 5. Depletion of Fap7 results in accumulation of incompletely assembled 43S preribosomes. (A) Fap7 depletion alters the sedimentation behavior of 43S preribosome-associated proteins. Extracts prepared from exponentially growing *GAL*::*3HA-FAP7* strains expressing TAP-tagged Rio2, Nob1, or Tsr1 (indicated on the right side of the panels) were fractionated by 10% to 50% sucrose density gradient centrifugation. Cells were either grown in YPG/R only (Undepleted) or grown in YPG/R and shifted to YPD for 5 h to deplete Fap7 (Depleted). The sedimentation of the TAP-tagged proteins was determined by Western blot analysis using the antibodies specific for the TAP tag. The positions of 40S and 60S subunits and of the 80S ribosomes/polysomes were determined by monitoring sedimentation of rRNAs in the gradient fractions by Northern analysis as shown in panel B. (B) The 20S pre-rRNA sediments at both 40S and 80S in Fap7-depleted cells. Northern blot analysis of RNA extracted from the sucrose gradient fractions is shown. The 25S rRNA was detected by hybridizing blots with radiolabeled oligonucleotide Y, whereas the 17S, 18S, and 20S rRNAs were detected using oligonucleotides B and A. (C) Fap7 depletion does not affect levels of Rio2, Tsr1, or Nob1 proteins. *GAL*::*3HA-FAP7* strains expressing TAP-tagged Nob1, Rio2, or Tsr1 were grown in YPG/R and shifted to YPD for 5 h to deplete Fap7. The TAP-tagged protein and 20S pre-rRNA levels were monitored 0, 2.5, and 5 h after the shift to YPD (Dex). Rio2-TAP, Tsr1-TAP, and Nob1-TAP proteins (indicated at the top of each lane) were detected by Western blot analysis using an antibody (PAP) specific for the TAP tag. Mpp10 was used as a loading control. The 20S pre-rRNA was detected by Northern blot analysis using probe B.

slightly smaller, perhaps partially degraded, 43S preribosomes, our results suggest that Fap7 depletion does not prevent association of Rio2, Nob1, and Tsr1 with 43S preribosomes.

We also determined whether the accumulation or stability of Rio2, Tsr1, or Nob1 was affected upon Fap7 depletion. We monitored the levels of the TAP-tagged proteins in *GAL*::*3HA-FAP7* strains 0, 2.5, and 5 h after the shift to YPD (Fig. 5C). In addition, as a control, we probed the blots for the SSU processome protein Mpp10. In all strains, the 3HA-tagged Fap7 protein was barely detectable 2.5 h after the shift to YPD; however, its absence did not dramatically affect the accumulation of Rio2, Tsr1, and Nob1 during 5 h of depletion. In contrast, a strong increase in 20S pre-rRNA levels was already clearly detectable after 2.5 h in YPD. Therefore, we conclude that Fap7 is not required for stable accumulation of these 43S preribosome protein components and that the increase in 20S pre-rRNA levels upon Fap7 depletion was not the result of codepletion of either Rio2, Tsr1, or Nob1.

Fap7 directly interacts with Rps14B in vitro. Recently, Jakovljevic et al. demonstrated that an arginine-to-alanine (R-to-A) substitution in the carboxy-terminal extension of the 40S ribosomal subunit protein Rps14B (Rps14B R134A) caused pre-rRNA-processing defects very similar to what we have

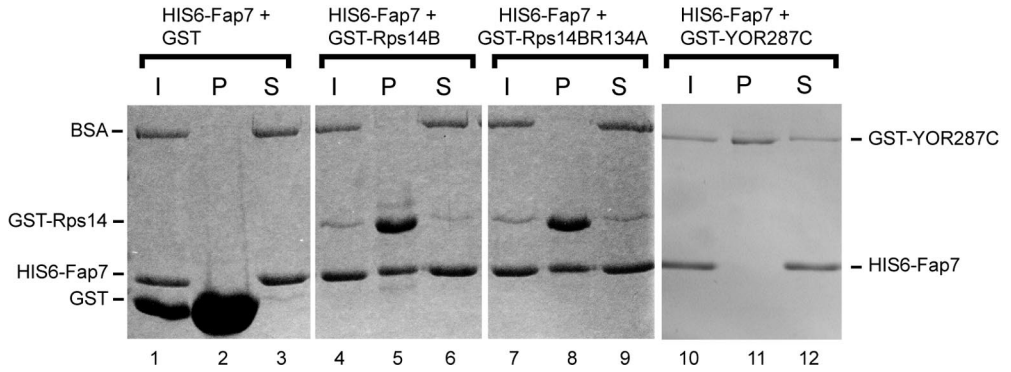

FIG. 6. Recombinant Fap7 directly interacts with wild-type and mutant (R134A) Rps14B proteins in GST pull-down assays. Six-histidine-tagged Fap7 and BSA were mixed with GST, GST-Rps14B, GST-Rps14B R134A, or GST-YOR287C and incubated on ice for 1 hour. Complexes were precipitated using glutathione-Sepharose beads and bound proteins (P) (lanes 2, 5, 8, and 11) were resolved by SDS-PAGE and stained with Coomassie brilliant blue. Ten percent of the input material (I) (lanes 1, 4, 7, and 10) and 10% of the supernatants (S) (lanes 3, 6, 9, and 12) were also analyzed.

observed in Fap7-depleted cells (22). This prompted us to test whether Fap7 interacts directly with Rps14. GST, GST-Rps14B wild-type and R134A mutant, and six-histidine-tagged Fap7 proteins were overexpressed in bacteria and purified to near homogeneity using ion exchange and affinity chromatography. Purified GST and GST-Rps14B proteins were incubated with six-histidine-tagged Fap7 and BSA, and complexes were allowed to form on ice. GST, BSA, and purified recombinant protein encoded by the open reading frame YOR287C were included as negative controls. BSA serves as a control because it has a pI of ~4.7, similar to that of Fap7 (4.35), and can be used to probe the likelihood of nonspecific electrostatic interactions determining Fap7 binding to Rps14. Likewise, the protein encoded by the YOR287C open reading frame will be positively charged at neutral pH (9.42 versus 11.28 for Rps14) and can be similarly used to probe the likelihood of nonspecific electrostatic interactions determining Rps14 binding to Fap7. Complexes were precipitated using glutathione-Sepharose beads, and bound proteins were resolved by SDS-PAGE and stained with Coomassie brilliant blue (Fig. 6 lanes 2, 5, 8, and 11 [lanes P]). Ten percent of the input material (Fig. 6, lanes I) and the supernatants after incubation with the beads were also analyzed (Fig. 6, lanes S). The results show that both the wild-type and the R134A Rps14B-GST fusion proteins efficiently bound recombinant Fap7 (Fig. 6, lanes 5 and 8) but not BSA. In addition, GST did not coprecipitate BSA or six-histidine-tagged Fap7 (Fig. 6, lane 2), and GST-YOR287C did not bind six-histidine-tagged Fap7 (Fig. 6, lane 11). These results not only demonstrate the specificity of the interaction but also suggest that the observed interactions between Fap7 and Rps14 are not simply the result of nonspecific electrostatic interactions. Thus, Fap7 directly binds to both Rps14B and the carboxy-terminal mutant in vitro.

To substantiate these results, we analyzed interactions between these proteins in the yeast two-hybrid assay. Unfortunately, overexpression of the Fap7 fusion proteins in combination with the Rps14B fusion proteins in yeast resulted in severe growth defects, irrespective of whether Fap7 was fused to the DNA-binding domain or the transcription activation domain (data not shown). We were therefore unable to determine interactions between these proteins in the yeast two-hybrid system.

Highly conserved residues implicated in NTPase activity and nucleotide binding are essential for Fap7 function and 20S pre-rRNA processing in vivo. Fap7 is predicted to belong to a family of P-loop-type kinases, which harbor putative Walker A and hhh(DE)XH-type Walker B motifs characteristic for NTPases (23, 28). The Walker A motif binds the β- and γ-phosphate moieties of nucleoside triphosphate (NTP), whereas the Walker B motif contacts the essential Mg^{2+} cofactor (47). Figure 7A shows an amino acid sequence alignment of Fap7 homologs identified in *Caenorhabditis elegans* (ceFap7), humans (TAF9/hFap7), and *Ashbya gossypii* (agFap7); the conserved putative enzymatic motifs are indicated. We analyzed whether highly conserved amino acids within the predicted enzymatic motifs were essential for Fap7 function in vivo. Wild-type and mutant *FAP7* genes were cloned into a plasmid under the control of the constitutive GPD promoter (p415GPD::*FAP7*). Mutations were made at the lysine at amino acid 20 in the Walker A motif (K20R in Fig. 7A and B); at a conserved lysine at amino acid 44, which is predicted to bind the α-phosphate of ribonucleoside substrates (28); and simultaneously at two highly conserved residues in the Walker B motif (D82AH84A in Fig. 7A and B). We also uncovered a stretch of amino acids that could correspond to a DXD motif that, like the Walker B motif, has the potential to function in coordinating Mg^{2+} binding (28) and mutated two conserved aspartic acid residues to alanines (D62AD64A in Fig. 7A and B). In addition, we tested a mutation identified in a temperature-sensitive *fap7-1* mutant strain (G19S in Fig. 7A and B) (23). We tested whether the mutated proteins could support growth in Fap7-depleted cells. Serial dilutions of cells expressing Fap7 mutant proteins or carrying empty vector were spotted on synthetic galactose (SG/R) (to verify even spotting of the culture) and synthetic dextrose (SD) solid media. Growth of the mutant strains was compared to growth of the *GAL*::*FAP7* strain expressing wild-type Fap7 protein from the same plasmid and to that of the same strain harboring an empty plasmid vector. Growth was monitored at 30°C (Fig. 7B). The strains dependent on the

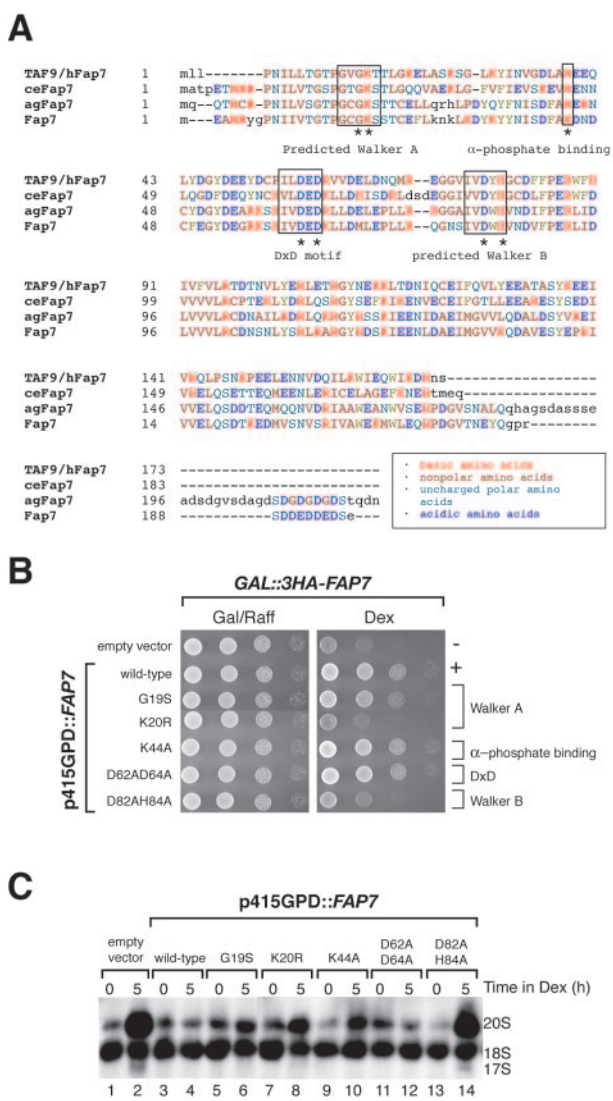

FIG. 7. The putative ATPase motif of Fap7 is essential for cell viability. (A) Multiple sequence alignment of Fap7 with homologs from *C. elegans* (ceFap7; E02H1.6), human (TAF9/hFap7; ENSP00000261565), and *A. gossypii* (agFap7; ACL150W) Fap7. The alignment was generated using the DiAlign program (www.genomatix.de/cgi-bin/dialign/dialign.pl). The amino acid positions relevant to the substitution mutants used in panels B and C are marked with asterisks, and an explanation of the color coding is shown on the bottom of the figure. (B) Conserved amino acids in the Walker A and B motifs are essential for Fap7 function in vivo. Serial dilutions (10-fold) of *GAL*::*3HA-FAP7* strains carrying p415GPD-*FAP7* wild-type and mutant genes were grown in synthetic galactose medium (SG/R-LEU) and spotted on either dextrose-containing plates (SD-LEU [Dex]) or galactose-containing plates (SG/R-LEU [Gal/Raff]). Results from a plate incubated at 30°C are shown. (C) Conserved amino acids in the Fap7 Walker A and B motifs are essential for 20S pre-rRNA processing and 18S rRNA synthesis in vivo. *GAL*::*3HA-FAP7* strains carrying p415GPD-*FAP7* wild-type and mutant genes or the empty vector were grown in synthetic galactose medium to exponential phase and subsequently shifted to synthetic dextrose medium for 5 hours to deplete Fap7. RNA was extracted from cells harvested before (0 h) and after (5 h) the shift to dextrose medium and was analyzed by Northern blot analysis. The 20S pre-rRNA and 18S rRNA were detected using oligonucleotides B and A, respectively.

K20R (Walker A motif) and D82AH84A (Walker B motif) mutant Fap7 proteins exhibited a significantly reduced growth rate compared to the strain expressing the wild-type Fap7 (Fig. 7B). Thus, these residues are important for Fap7 function. In contrast, the Walker A G19S mutation, the K44A, and the mutations in the putative DXD motif (D62AD64A) supported growth as well as the wild-type Fap7 allele, demonstrating that these residues are not important for Fap7 function in vivo (Fig. 7B).

We next analyzed the effect of these mutations in Fap7 on the processing of the 20S pre-rRNA and 18S rRNA synthesis. *GAL*::*3HA-FAP7* strains expressing the various Fap7 mutants were grown in YPG/R media to exponential phase and subsequently grown in dextrose-containing medium (YPD) for 5 h to deplete Fap7. Total RNA extracted from cells harvested before and 5 h after the shift to YPD was subjected to Northern blot analysis to detect the 20S pre-rRNA and the mature 18S rRNA. The results show that 5 h after the shift to YPD, Fap7-depleted strains harboring the empty vector or expressing plasmid-encoded Fap7 K20R (Walker A) mutant and the D82AH84A (Walker B) mutant showed reduced 18S rRNA levels and accumulated the 20S pre-rRNA (Fig. 7C, lanes 2, 8, and 14). In some lanes, we also detected a faint band migrating below the 18S rRNA, which may correspond to the 17S degradation product (Fig. 7C, lanes 2 and 14). In contrast, the plasmids encoding wild-type, G19S, and K44A Fap7 alleles largely restored 20S pre-rRNA processing and 18S rRNA synthesis in Fap7-depleted strains (Fig. 7C, lanes 3 to 6 and 9 to 12). Notably, while the G19S Fap7 mutant complemented growth on solid media as well as the wild-type allele did (Fig. 7B), we noticed a modest accumulation of the 20S pre-rRNA and slightly lower 18S rRNA levels in liquid media (Fig. 7C, lanes 5 and 6).

Consistent with the idea that Fap7 has NTPase activity in vivo, conserved amino acids predicted to be involved in nucleotide binding and NTPase activity are essential for Fap7 function and required for 20S pre-rRNA processing.

DISCUSSION

Using two different methods, we have shown that Fap7 is required for processing of the 20S pre-rRNA at site D but not at other pre-rRNA-processing steps. Consistent with a role in SSU synthesis, sucrose gradient centrifugation experiments demonstrated reduced levels of the SSU and an increase in the level of free LSU in Fap7-depleted cells. By FISH, we determined that Fap7-depleted cells accumulate the 20S pre-rRNA in the cytoplasm, suggesting that Fap7 is not involved in nuclear export of the 20S pre-rRNA (and thus 43S preribosomes) but is required for cleavage at site D in the cytoplasm. Consistent with its predicted NTPase activity, we have demonstrated that the conserved lysine in the Walker A motif and conserved residues in the Walker B motif are critical for Fap7 function and required for 20S pre-rRNA processing in vivo. We propose a model in which Fap7 regulates NTP-dependent cleavage of the 20S pre-rRNA at site D in the cytoplasm by directly binding to Rps14.

Cleavage of the 20S pre-rRNA at site D involves transient association between Fap7 and 43S preribosomes. The amount of accumulated 20S pre-rRNA in Fap7-depleted cells is remarkable, as it is increased 20 times over undepleted cells and

is approximately equal to the amount of mature 18S rRNA. In addition, accumulation of other pre-rRNAs does not occur. Numerous nonribosomal (Drs2, Rrp12, Rio1, Rio2, Tsr1, Tsr2, Nob1) and ribosomal (Rps0, Rps21/Ubi3, Rps14) proteins have previously been shown to be important for efficient 20S pre-rRNA processing (6, 9, 10, 16, 22, 34, 35, 38, 44). In most cases, however, a mild delay in site D processing was observed, resulting in only a two- to fivefold increase in 20S pre-rRNA levels. Also, earlier processing steps were generally affected to some extent (9, 10, 16, 34, 35, 44).

Interestingly, in Fap7-depleted cells, the 20S pre-rRNA was detectable in fractions corresponding to 40S (likely representing the 43S) and 80S. The detection of the 20S pre-rRNA in ribosome-sized complexes suggests that the 43S preribosome can associate with the mature LSU to make an 80S ribosome. This ribosome, containing the immature 20S pre-rRNA, is nonfunctional (43). However, it is intriguing to speculate that the final cleavage step (D) in the generation of the mature 3′ end of the 18S rRNA can occur in the 80S ribosome. This possibility is strengthened by the observation that in normally growing cells, Nob1, Fap7, and a small amount of the 20S pre-rRNA cosediment with 80S ribosomes but not with polyribosomes (6 and this work). Furthermore, *Dictyostelium discoideum* preribosomes are often detected in 80S monosomes and even polyribosomes in vivo and in vitro (31, 32). In this organism, the assembly of immature ribosomal subunits into polyribosomes is an obligatory step, and it has been shown that if newly formed ribosomes cannot function in translation, late rRNA maturation steps do not take place (31). Thus, it is tempting to speculate that rRNA processing is a quality control step in ribosome biogenesis.

While we have demonstrated that Fap7 is not required for nuclear export of 43S preribosomes, from our studies we cannot discriminate whether Fap7 binds Rps14 in the nucleus or in the cytoplasm. Its nuclear and cytoplasmic localizations (21, 23) suggest that Fap7 may associate with 43S preribosomes in the nucleus and is then exported to the cytoplasm as part of these 20S-containing complexes.

The SSU protein Rps14 recruits Fap7 to 43S preribosomes to facilitate site D cleavage. Our combined results suggest a model in which Fap7 is recruited to 43S preribosomes via Rps14. This model is based on our pull-down experiments, which demonstrated that recombinant Fap7 directly binds GST-Rps14 efficiently in vitro. In addition, the *Drosophila melanogaster* Fap7 and Rps14 homologs were shown to directly interact in the yeast two-hybrid system (17), demonstrating that this functional interaction is evolutionary conserved.

The SSU protein Rps14, the yeast homolog of the bacterial S11 protein, directly binds helix 28 of 18S rRNA and is essential for the assembly of 40S ribosomal subunits (27, 33). Like the bacterial S11 protein, yeast Rps14 contains a basic carboxy-terminal tail that plays an important role in binding to rRNA (1). In three-dimensional reconstructions of the yeast 40S ribosomal subunit, the Rps14 carboxy-terminal tail has been modeled in close proximity to the 3′ end of the 18S rRNA (22, 41). Since it is unlikely that Rps14 itself has nuclease activity, it has been proposed that it may play an important role in recruiting processing factors, such as an endonuclease, to the processing site (22). This suggests Fap7 interacts with the 43S preribosome close to the D cleavage site. Interestingly, in the yeast three-hybrid system, the *rps14 R134A* mutant has severely diminished rRNA-binding activity (1). While this mutation does not affect Rps14 binding to Fap7 in vitro, it weakens Rps14 association with 43S ribosomal subunits in vivo (22). Indeed, the results that we obtained upon Fap7 depletion are remarkably similar to what has been described for the *rps14B R134A* mutant strain (22). Therefore, a plausible explanation for the 20S pre-rRNA-processing defect observed in this *rps14B* mutant strain is that Fap7 cannot efficiently interact with 43S preribosomes because of a lack of Rps14 in these particles.

The putative NTPase motifs are essential for Fap7 function in vivo. We have presented genetic evidence suggesting Fap7 may function as an NTPase in vivo because the highly conserved lysine in the Walker A motif and two conserved residues in the Walker B motif are essential for Fap7 function and 20S pre-rRNA processing in vivo. In addition, it has been shown previously that amino acids G19 and S21 in the Walker A motif are important for cell viability (23). Notably, none of the mutations were dominant negative when overexpressed in a wild-type background (data not shown).

Because it has been proposed that Fap7 belongs to a family of P-loop kinases that is related to the ribonucleoside kinases (28), we tested whether highly purified recombinant Fap7 has NTPase and ribonucleoside kinase activity in vitro under a broad range of conditions (data not shown). These included increasing salt concentrations (30 to 300 mM KCl), increasing pH values (6.5 to 8.8), different cations ($MgCl_2$, $CaCl_2$, $ZnCl_2$, $MnCl_2$) and increasing cation concentrations (0.5 mM to 10 mM). Unfortunately, recombinant Fap7 did not demonstrate any significant ATPase/GTPase or ribonucleoside kinase activity under any of the conditions tested or in the presence or absence of mono- or dinucleoside substrates. Addition of total yeast RNA, partially purified 43S preribosomes, or recombinant Rps14B proteins failed to activate or stimulate Fap7 NTPase activity. Finally, we purified Fap7 from yeast using TAP (see Fig. S2 in the supplemental material) (37). Unfortunately, this purified Fap7 also did not show significant NTPase activity in vitro (data not shown). However, it is conceivable that our in vitro system lacked essential cofactors or that we did not test the optimal substrates.

What is the elusive nuclease responsible for cleavage at site D? It has been proposed that Nob1 is the endonuclease that carries out the cleavage at site D in the cytoplasm, because it bears a PIN domain. This is supported by genetic and in silico studies (6, 8); however, in vitro enzymatic activities have not been explored. The known endo- and exonucleases involved in ribosome biogenesis, including the RNase MRP complex and numerous exonucleases, are not detected in purified preribosomes, suggesting that these enzymes transiently interact with the complexes (reviewed in references 7, 19, and 42). If Nob1 is the endonuclease, it is unusual in that it is stably associated with preribosomes. Indeed, Nob1 remains stably associated with 43S preribosomes even in Fap7-depleted cells (reference 6 and this work). Thus, the block in cleavage at site D in this strain cannot be caused by a lack of Nob1. However, we cannot rule out the possibility that Nob1 and Fap7, both of which have enzymatic motifs, function together in cleavage at site D.

From our results, it is tantalizing to speculate that Fap7 is the elusive endonuclease responsible for cleavage at site D. First, as one might expect from a nuclease, Fap7 likely tran-

siently associates with 43S preribosomes that contain the pre-18S rRNA substrate. Second, Fap7 directly binds Rps14 in vitro, suggesting that it binds the 43S preribosomes in close proximity to the cleavage site. Third, it is a putative NTPase, and it is likely that NTP hydrolysis is necessary to fuel the cleavage reaction. Although Fap7 does not contain a previously described endonuclease domain, such a domain cannot always be predicted from the amino acid sequence, as has been shown for the endonuclease Argonaute, which functions in RNA interference (40).

ACKNOWLEDGMENTS

We are grateful to Jelena Jakovljevic and John Woolford for providing Rps14 DNA constructs and helpful suggestions. We thank Sandra Wolin for helpful discussions and members of our laboratory for critically reading the manuscript. We are grateful to Patrick Sung and all the members of his laboratory for help with protein purifications and providing reagents and their facilities.

This work was supported by Leslie H. Warner and Anna Fuller Postdoctoral Cancer Research fellowships (S.G.), and the National Institutes of Health (GM52581).

REFERENCES

1. **Antunez de Mayolo, P., and J. L. Woolford, Jr.** 2003. Interactions of yeast ribosomal protein rpS14 with RNA. J. Mol. Biol. **333:**697–709.
2. **Arcus, V. L., K. Backbro, A. Roos, E. L. Daniel, and E. N. Baker.** 2004. Distant structural homology leads to the functional characterization of an archaeal PIN domain as an exonuclease. J. Biol. Chem. **279:**16471–16478.
3. **Brand, R. C., J. Klootwijk, T. J. Van Steenbergen, A. J. De Kok, and R. J. Planta.** 1977. Secondary methylation of yeast ribosomal precursor RNA. Eur. J. Biochem. **75:**311–318.
4. **Dragon, F., J. E. Gallagher, P. A. Compagnone-Post, B. M. Mitchell, K. A. Porwancher, K. A. Wehner, S. Wormsley, R. E. Settlage, J. Shabanowitz, Y. Osheim, A. L. Beyer, D. F. Hunt, and S. J. Baserga.** 2002. A large nucleolar U3 ribonucleoprotein required for 18S ribosomal RNA biogenesis. Nature **417:**967–970.
5. **Dunbar, D. A., S. Wormsley, T. M. Agentis, and S. J. Baserga.** 1997. Mpp10p, a U3 small nucleolar ribonucleoprotein component required for pre-18S rRNA processing in yeast. Mol. Cell. Biol. **17:**5803–5812.
6. **Fatica, A., M. Oeffinger, M. Dlakic, and D. Tollervey.** 2003. Nob1p is required for cleavage of the 3′ end of 18S rRNA. Mol. Cell. Biol. **23:**1798–1807.
7. **Fatica, A., and D. Tollervey.** 2002. Making ribosomes. Curr. Opin. Cell Biol. **14:**313–318.
8. **Fatica, A., D. Tollervey, and M. Dlakic.** 2004. PIN domain of Nob1p is required for D-site cleavage in 20S pre-rRNA. RNA **10:**1431–1436.
9. **Finley, D., B. Bartel, and A. Varshavsky.** 1989. The tails of ubiquitin precursors are ribosomal proteins whose fusion to ubiquitin facilitates ribosome biogenesis. Nature **338:**394–401.
10. **Ford, C. L., L. Randal-Whitis, and S. R. Ellis.** 1999. Yeast proteins related to the p40/laminin receptor precursor are required for 20S ribosomal RNA processing and the maturation of 40S ribosomal subunits. Cancer Res. **59:**704–710.
11. **Fromont-Racine, M., B. Senger, C. Saveanu, and F. Fasiolo.** 2003. Ribosome assembly in eukaryotes. Gene **313:**17–42.
12. **Gallagher, J. E., D. A. Dunbar, S. Granneman, B. M. Mitchell, Y. Osheim, A. L. Beyer, and S. J. Baserga.** 2004. RNA polymerase I transcription and pre-rRNA processing are linked by specific SSU processome components. Genes Dev. **18:**2506–2517.
13. Reference deleted.
14. **Gavin, A. C., M. Bosche, R. Krause, P. Grandi, M. Marzioch, A. Bauer, J. Schultz, J. M. Rick, A. M. Michon, C. M. Cruciat, M. Remor, C. Hofert, M. Schelder, M. Brajenovic, H. Ruffner, A. Merino, K. Klein, M. Hudak, D. Dickson, T. Rudi, V. Gnau, A. Bauch, S. Bastuck, B. Huhse, C. Leutwein, M. A. Heurtier, R. R. Copley, A. Edelmann, E. Querfurth, V. Rybin, G. Drewes, M. Raida, T. Bouwmeester, P. Bork, B. Seraphin, B. Kuster, G. Neubauer, and G. Superti-Furga.** 2002. Functional organization of the yeast proteome by systematic analysis of protein complexes. Nature **415:**141–147.
15. **Geerlings, T. H., A. W. Faber, M. D. Bister, J. C. Vos, and H. A. Raue.** 2003. Rio2p, an evolutionarily conserved, low abundant protein kinase essential for processing of 20S pre-rRNA in *Saccharomyces cerevisiae*. J. Biol. Chem. **278:**22537–22545.
16. **Gelperin, D., L. Horton, J. Beckman, J. Hensold, and S. K. Lemmon.** 2001. Bms1p, a novel GTP-binding protein, and the related Tsr1p are required for distinct steps of 40S ribosome biogenesis in yeast. RNA **7:**1268–1283.
17. **Giot, L., J. S. Bader, C. Brouwer, A. Chaudhuri, B. Kuang, Y. Li, Y. L. Hao, C. E. Ooi, B. Godwin, E. Vitols, G. Vijayadamodar, P. Pochart, H. Machineni, M. Welsh, Y. Kong, B. Zerhusen, R. Malcolm, Z. Varrone, A. Collis, M. Minto, S. Burgess, L. McDaniel, E. Stimpson, F. Spriggs, J. Williams, K. Neurath, N. Ioime, M. Agee, E. Voss, K. Furtak, R. Renzulli, N. Aanensen, S. Carrolla, E. Bickelhaupt, Y. Lazovatsky, A. DaSilva, J. Zhong, C. A. Stanyon, R. L. Finley, Jr., K. P. White, M. Braverman, T. Jarvie, S. Gold, M. Leach, J. Knight, R. A. Shimkets, M. P. McKenna, J. Chant, and J. M. Rothberg.** 2003. A protein interaction map of *Drosophila melanogaster*. Science **302:**1727–1736.
18. **Grandi, P., V. Rybin, J. Bassler, E. Petfalski, D. Strauss, M. Marzioch, T. Schäfer, B. Kuster, H. Tschochner, D. Tollervey, A. C. Gavin, and E. Hurt.** 2002. 90S pre-ribosomes include the 35S pre-rRNA, the U3 snoRNP, and 40S subunit processing factors but predominantly lack 60S synthesis factors. Mol. Cell **10:**105–115.
19. **Granneman, S., and S. J. Baserga.** 2004. Ribosome biogenesis: of knobs and RNA processing. Exp. Cell Res. **296:**43–50.
20. **Huh, W., J. V. Falvo, L. C. Gerke, A. S. Carroll, R. W. Howson, J. S. Weissman, and E. K. O'Shea.** 2003. Global analysis of protein localization in budding yeast. Nature **425:**686–691.
21. **Ito, T., T. Chiba, R. Ozawa, M. Yoshida, M. Hattori, and Y. Sakaki.** 2001. A comprehensive two-hybrid analysis to explore the yeast protein interactome. Proc. Natl. Acad. Sci. USA **98:**4569–4574.
22. **Jakovljevic, J., P. Antunez de Mayolo, T. D. Miles, T. M. L. Nguyen, I. Leger-Silvestre, N. Gas, and J. L. Woolford, Jr.** 2004. The carboxy-terminal extension of yeast ribosomal protein S14 is necessary for maturation of 43S pre-ribosomes. Mol. Cell **14:**331–342.
23. **Juhnke, H., C. Charizanis, F. Latifi, B. Krems, and K. D. Entian.** 2000. The essential protein Fap7 is involved in the oxidative stress response of *Saccharomyces cerevisiae*. Mol. Microbiol. **34:**936–949.
24. **Kufel, J., B. Dichtl, and D. Tollervey.** 1999. Yeast Rnt1p is required for cleavage of the pre-ribosomal RNA in the 3′ ETS but not the 5′ ETS. RNA **5:**909–917.
25. **Lafontaine, D., J. Delcour, A. L. Glasser, J. Desgres, and J. Vandenhaute.** 1994. The DIM1 gene responsible for the conserved m6(2)Am6(2)A dimethylation in the 3′-terminal loop of 18 S rRNA is essential in yeast. J. Mol. Biol. **241:**492–497.
26. **Lafontaine, D. L., T. Preiss, and D. Tollervey.** 1998. Yeast 18S rRNA dimethylase Dim1p: a quality control mechanism in ribosome synthesis? Mol. Cell. Biol. **18:**2360–2370.
27. **Larkin, J. C., J. R. Thompson, and J. L. Woolford, Jr.** 1987. Structure and expression of the *Saccharomyces cerevisiae* CRY1 gene: a highly conserved ribosomal protein gene. Mol. Cell. Biol. **7:**1764–1775.
28. **Leipe, D. D., E. V. Koonin, and L. Aravind.** 2003. Evolution and classification of P-loop kinases and related proteins. J. Mol. Biol. **333:**781–815.
29. **Longtine, M. S., A. McKenzie, D. J. Demarini, N. G. Shah, A. Wach, A. Brachat, P. Philippsen, and J. R. Pringle.** 1998. Additional modules for versatile and economical PCR-based gene deletion and modification in *Saccharomyces cerevisiae*. Yeast **14:**953–961.
30. **Lygerou, Z., C. Allmang, D. Tollervey, and B. Seraphin.** 1996. Accurate processing of a eukaryotic precursor ribosomal RNA by ribonuclease MRP in vitro. Science **272:**268–270.
31. **Mangiarotti, G., and S. Chiaberge.** 1997. Reconstitution of functional eukaryotic ribosomes from *Dictyostelium discoideum* ribosomal proteins and RNA. J. Biol. Chem. **272:**19682–19687.
32. **Mangiarotti, G., S. Chiaberge, and S. Bulfone.** 1997. rRNA maturation as a "quality" control step in ribosomal subunit assembly in *Dictyostelium discoideum*. J. Biol. Chem. **272:**27818–27822.
33. **Moritz, M., A. G. Paulovich, Y. F. Tsay, and J. L. Woolford, Jr.** 1990. Depletion of yeast ribosomal proteins L16 or rp59 disrupts ribosome assembly. J. Cell Biol. **111:**2261–2274.
34. **Oeffinger, M., M. Dlakic, and D. Tollervey.** 2004. A pre-ribosome-associated HEAT-repeat protein is required for export of both ribosomal subunits. Genes Dev. **18:**196–209.
35. **Peng, W. T., M. D. Robinson, S. Mnaimneh, N. J. Krogan, G. Cagney, Q. Morris, A. P. Davierwala, J. Grigull, X. Yang, W. Zhang, N. Mitsakakis, O. W. Ryan, N. Datta, V. Jojic, C. Pal, V. Canadien, D. Richards, B. Beattie, L. F. Wu, S. J. Altschuler, S. Roweis, B. J. Frey, A. Emili, J. F. Greenblatt, and T. R. Hughes.** 2003. A panoramic view of yeast noncoding RNA processing. Cell **113:**919–933.
36. **Raue, H. A.** 2004. Pre-ribosomal RNA processing and assembly in *Saccharomyces cerevisiae*, p. 199–222. *In* M. O. Olson (ed.), The nucleolus. Kluwer Academic/Plenum Publishers, New York, N.Y.
37. **Rigaut, G., A. Shevchenko, B. Rutz, M. Wilm, M. Mann, and B. Séraphin.** 1999. A generic protein purification method for protein complex characterization and proteome exploration. Nat. Biotechnol. **17:**1030–1032.
38. **Ripmaster, T. L., G. P. Vaughn, and J. L. Woolford, Jr.** 1993. DRS1 to DRS7, novel genes required for ribosome assembly and function in *Saccharomyces cerevisiae*. Mol. Cell. Biol. **13:**7901–7912.
39. **Schäfer, T., D. Strauss, E. Petfalski, D. Tollervey, and E. Hurt.** 2003. The path from nucleolar 90S to cytoplasmic 40S pre-ribosomes. EMBO J. **22:**1370–1380.
40. **Song, J. J., S. K. Smith, G. J. Hannon, and L. Joshua-Tor.** 2004. Crystal structure of Argonaute and its implications for RISC slicer activity. Science **305:**1434–1437.

41. **Spahn, C. M., R. Beckmann, N. Eswar, P. A. Penczek, A. Sali, G. Blobel, and J. Frank.** 2001. Structure of the 80S ribosome from Saccharomyces cerevisiae—tRNA-ribosome and subunit-subunit interactions. Cell **107:**373–386.
42. **Tschochner, H., and E. Hurt.** 2003. Pre-ribosomes on the road from the nucleolus to the cytoplasm. Trends Cell Biol. **13:**255–263.
43. **Udem, S. A., and J. R. Warner.** 1973. The cytoplasmic maturation of a ribosomal precursor ribonucleic acid in yeast. J. Biol. Chem. **248:**1412–1416.
44. **Vanrobays, E., J. P. Gelugne, P. E. Gleizes, and M. Caizergues-Ferrer.** 2003. Late cytoplasmic maturation of the small subunit requires RIO proteins in *Saccharomyces cerevisiae*. Mol. Cell. Biol. **23:**2083–2095.
45. **Vanrobays, E., P. E. Gleizes, C. Bousquet-Antonelli, J. Noaillac-Depeyre, M. Caizergues-Ferrer, and J. P. Gelugne.** 2001. Processing of 20S pre-rRNA to 18S ribosomal RNA in yeast requires Rrp10p, an essential non-ribosomal cytoplasmic protein. EMBO J. **20:**4204–4213.
46. **Venema, J., and D. Tollervey.** 1999. Ribosome synthesis in Saccharomyces cerevisiae. Annu. Rev. Genet. **33:**261–311.
47. **Walker, J. E., M. Saraste, M. J. Runswick, and N. J. Gay.** 1982. Distantly related sequences in the alpha-and beta-subunits of ATP synthase, myosin kinases and other ATP-requiring enzymes and a common nucleotide binding fold. EMBO J. **1:**945–951.
48. **Wehner, K. A., and S. J. Baserga.** 2002. The sigma(70)-like motif: a eukaryotic RNA binding domain unique to a superfamily of proteins required for ribosome biogenesis. Mol. Cell **9:**329–339.